Moveout formulas for a curved 2D measurement surface and near-zero-offset primary reflections: theory and applications

P. Chira and P. Hubral

email: *Pedro.Chira@gpi.uni-karlsruhe*

keywords: *Analytic moveout formulas, curved measurement surface*

ABSTRACT

Analytic moveout formulas for primary near-zero-offset reflections in various types of gathers play a significant role in the seismic reflection method. They are required in stacking methods, e.g. the common midpoint (CMP) or the Common-Reflection-Surface (CRS) stack. They also play a very important role in Dix-type traveltime inversions. They are particularly attractive, if they can be given a "physical" or "quasi-physical" interpretation, involving for instance the wavefront curvatures of specific waves. The formulas presented here have such a form. They give particular attention to the influence that a curved measurement surface has on the computation of the traveltime and the moveout in various gathers as well as on the normal-moveout (NMO) velocity in the CMP gather. This influence should be accounted for in the CMP or CRS stack as well as in the Dix-type inversion. In the computation of interval velocities and the recovery of the depth of reflectors, this new NMO velocity formula is more suited than the root-mean-square (rms) or NMO velocities for planar measurement surfaces.

INTRODUCTION

Analytic moveout formulas have a long tradition of being applied in the seismic reflection method (Dürbaum, 1954; Dix, 1955; Shah, 1973; Fomel and Grechka, 1998). Particularly in the light of "Macro-model-independent reflection imaging" (Hubral, 1999) analytic moveout formulas in midpoint (m) and half-offset (h) coordinates have gained a new importance in such stacking processes as the Polystack (de Bazelaire, 1988; de Bazelaire and Viallix, 1994) and Multifocusing (Gelchinsky et al., 1999a,b). Here we generalize the so-called Zero-Offset (ZO) Common-Reflection-Surface (CRS) stack formula, which is used to simulate zero-offset sections from prestack data in a data-driven macrovelocity model independent way (Müller et al., 1998; Jäger et al., 2001). The proposed generalized CRS stack moveout formula is formulated in such a way that the influence of the curved measurement surface can be clearly recognized.

THEORY

According to Schleicher et al. (1993), the hyperbolic traveltime approximation for a paraxial ray from S' to R' and from R' to G', both on a curved measurement surface, in the vicinity of a normal (zero-offset) ray from SG to R and from R to SG (Figure 1a) is given by

$$t_{hyp}^2(m,h) = (t_0 - 2\,p_0\,m)^2 + 2\,t_0\,[(B^{-1}\,A - B^{-1})\,m^2 + (\,B^{-1}\,A + B^{-1})\,h^2] \qquad (1)$$

with

$$p_0 = \frac{-\sin\beta_S{}^*}{v_1}\,, \quad m = \frac{x_S + x_G}{2}\,, \quad h = \frac{x_G - x_S}{2}\,. \qquad (2)$$

$$A = \frac{1}{K_{NIP} - K_N}\,\left(K_{NIP} + K_N - \frac{2\,K_S}{\cos\beta_S{}^*}\right)\,, \qquad (3a)$$

$$B = \frac{1}{K_{NIP} - K_N}\,\left(\frac{2\,v_1}{\cos^2\beta_S{}^*}\right)\,, \qquad (3b)$$

$$C = \frac{1}{K_{NIP} - K_N}\left(\frac{2\,K_{NIP}\,K_N\cos^2\beta_S{}^*}{v_1} + \frac{2\,K_S^2}{v_1} - 2(K_{NIP} + K_N)\frac{\cos\beta_S{}^* K_S}{v_1}\right)\,, \qquad (3c)$$

$$D = \frac{1}{K_{NIP} - K_N}\,\left(K_{NIP} + K_N - \frac{2\,K_S}{\cos\beta_S{}^*}\right)\,. \qquad (3d)$$

Formula (1) is valid for a 2D laterally inhomogeneous medium. v_1 is the near-surface velocity at the ZO location SG, t_0 is the zero-offset (two-way) traveltime. x_S and x_G are the coordinates of the projections of the source S' and receiver G' measured along the x_1-axis tangent to the curved surface and with the origin at SG. m is the midpoint and h is the half-offset on that tangent. $\beta_S{}^*$ is the angle of incidence of the normal ray (emerging on the curved measurement surface at SG) with the normal to the tangent at SG (see Figures 1b and 2).

$A\,, B\,, C$ and D (Chira and Hubral, 2001) are the components of the so-called 2×2 surface-to-surface propagator matrix $\mathbf{T}$ (Bortfeld, 1989; Červený, 2001) for the two-way normal ray. K_S is the surface curvature at the point SG. K_{NIP} and K_N are the curvatures of the emerging hypothetical "Normal-Incidence-Point (NIP)-wave" and the "Normal (N) wave" observed at SG, respectively (Hubral, 1983; Jäger et al., 2001). The NIP wave is associated with a point source exploding at the normal incidence point (NIP) R. The N-wave results in an exploding reflector experiment.

Inserting eqs. (2), (3a), and (3b) into eq. (1) we obtain

$$t_{hyp}^2(m,h) = \left(t_0 + 2\,\frac{\sin\beta_S{}^*}{v_1}\,m\right)^2 + \frac{2\,t_0}{v_1}\,\left(K_N\,\cos^2\beta_S^* - \cos\beta_S^*\,K_S\right)\,m^2 + \frac{2\,t_0}{v_1}\,\left(K_{NIP}\,\cos^2\beta_S^* - \cos\beta_S^*\,K_S\right)\,h^2\,. \qquad (4)$$

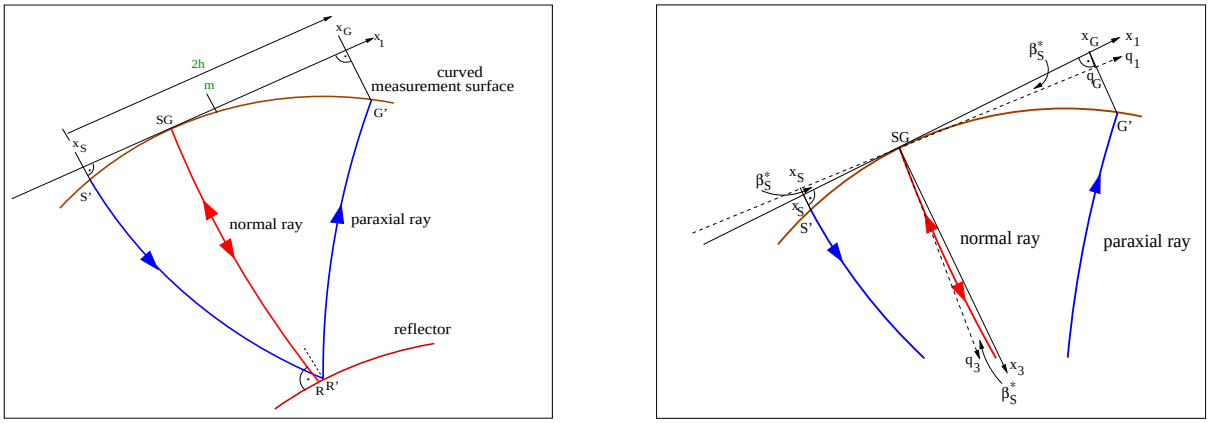

(a) **(b)**

Figure 1: a) Ray diagram for a paraxial ray in the vicinity of a normal (central) ray in a 2D laterally inhomogeneous medium. b) Blow-up of Figure 1(a) showing the (x_1, x_3) 2D local and (q_1, q_3) ray-centered (dashed) coordinate systems at SG.

Given $P_0(x_{SG} = 0, t_0)$, K_S and v_1 (x_{SG} is the coordinate of the point SG in the x_1 axis), the triplet $(\beta_S^*,\ K_{NIP},\ K_N)$ can be looked upon as the searched-for kinematic parameters in the prestack data. They help to solve a variety of stacking and inversion problems (Hubral, 1999). They can be obtained by using the presently existing 2D CRS stack (Jäger et al., 2001) that results from eq. (4) by substituting $K_S = 0$.

Particular cases

We present three particular reductions of formula (4), which are part of the strategy to search the three parameters at P_0.

Common midpoint (CMP) gather

For this case ($m = 0$) the equation (4) reduces to

$$t_{CMP}^2(h) = t_0^2 + \frac{2\ t_0}{v_1}\ \left(K_{NIP}\ \cos^2\beta_S^* - \cos\beta_S^*\ K_S\right)\ h^2\ . \tag{5}$$

This expression is commonly written as (Shah, 1973)

$$t_{CMP}^2(h) = t_0^2 + \frac{4\ h^2}{v_{NMO}^2}\ , \tag{6}$$

where the NMO velocity v_{NMO} is given by

$$v_{NMO}^2 = \frac{2\ v_1}{t_0\ \left(K_{NIP}\ \cos^2\beta_S^* - \cos\beta_S^*\ K_S\right)}\ . \tag{7}$$

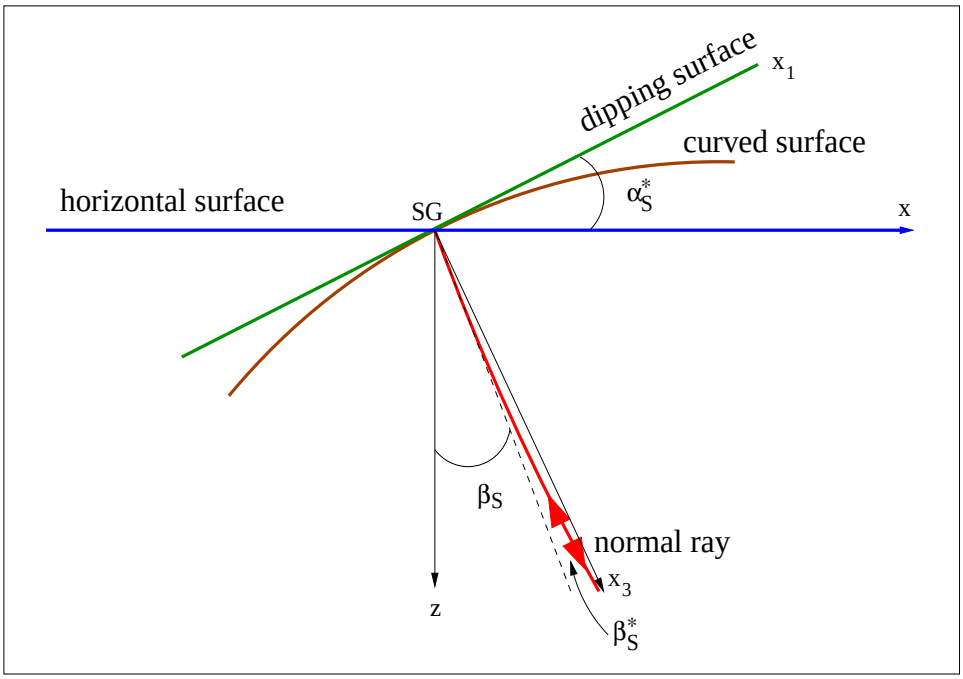

Figure 2: The relationship between curved, dipping and horizontal surfaces.

For $K_S = 0$ this reduces to Shah's formula. For a 1-D layered model with a planar horizontal measurement surface, straight vertical normal ray and incidence angle $\beta_S^* = 0$ this expression reduces to $v_{NMO} = v_{rms}$, where v_{rms} is the familiar rms velocity (Dix, 1955).

Common shot (CS) gather

For this case ($x_S = 0$) the equation (4) reduces to

$$t_{CS}^2(x_G) = \left(t_0 + \frac{\sin\beta_S{}^*}{v_1}\, x_G\right)^2 + \frac{t_0}{2\,v_1}\,\left(K_N\,\cos^2\beta_S^* + K_{NIP}\,\cos^2\beta_S^* - 2\cos\beta_S^*\,K_S\right)\,{x_G}^2\,, \tag{8}$$

where according to Hubral (1983) and Chira and Hubral (2001), we have $K_{NIP} + K_N = 2\,K_0$, with K_0 being the wavefront curvature of the reflected wave that originated from a point source at SG.

Zero-Offset (ZO) gather

Let us consider coincident shot-receiver pairs at the curved measurement surface and approximate the zero-offset reflections in the vicinity of SG. For this case ($h = 0$) the equation (4) reduces to

$$t_{ZO}^2(m) = \left(t_0 + 2\,\frac{\sin\beta_S{}^*}{v_1}\,m\right)^2 + \frac{2\,t_0}{v_1}\,\left(K_N\,\cos^2\beta_S^* - \cos\beta_S^*\,K_S\right)\,m^2\,. \tag{9}$$

All three formulas (7 to 9) should be considered in the 2D CRS stack according to Jäger et al. (2001) for a curved measurement surface.

TRANSFORMED MEASUREMENT SURFACES

The moveout formula (4) can be simply transformed to that which would result if the curved measurement surface at SG would be replaced by the tangent, i.e. the planar dipping surface at point SG. This would be achieved by substituting $K_S = 0$. It could be further reduced to a formula, which would result for a horizontal measurement surface passing through SG by using the dip angle α_S^* of the measurement surface at SG and replacing β_S^* by $\beta_S = \beta_S^* - \alpha_S^*$ (Figure 2). β_S is the angle between the emerging normal ray and the normal to the horizontal surface.

APPLICATIONS

Let us assume that the coherency-based CRS stack search strategy, based on applying formula (4) to $P_0(x_{SG} = 0, t_0)$, has provided for every primary reflection from each subsurface reflector the three kinematic attributes $(\beta_S^*,\ K_{NIP},\ K_N)$. We can then consider their following applications.

Zero-offset CRS stack for a curved measurement surface

The attributes can be substituted into eq. (4) to perform a 3-parameter zero-offset CRS stack to simulate from the prestack data a zero-offset trace at each point SG on the curved measurement surface.

The Figure (3) shows a 2D model consisting of three constant velocity layers with curved interfaces. The normal ray corresponding to $X_0 = 1.00$ km, it passes through the medium and reflects on the second (dome-like) interface.
In the Figure (3) the ZO CRS stack operator (black surface) approximates the primary reflection events in the vicinity of the central point P_0 which corresponds to the central (normal) ray. To perform the ZO CRS stack, we stack along the ZO CRS stack operator (eq. 4) and assign the stacked value to the point P_0. For further details on the implementation of zero-offset CRS stack see Jäger et al. (2001).

Dix-type traveltime inversions

Without making any assumptions on the velocity model or subsurface reflectors, we can easily transform all kinematic attributes obtained for the curved measurement surface to those, which would result for the planar dipping or horizontal surface (Figure 2). The NMO velocity (7) can then be changed to that of the tangent dipping measurement surface at SG

$$v_{NMO,T}^2 = \frac{2\ v_1}{t_0\ K_{NIP}\ \cos^2\beta_S^*}\,. \tag{10}$$

It can also be changed to that of the horizontal measurement surface at SG

$$v_{NMO,H}^2 = \frac{2\ v_1}{t_0\ K_{NIP}\ \cos^2\beta_S}\,. \tag{11}$$

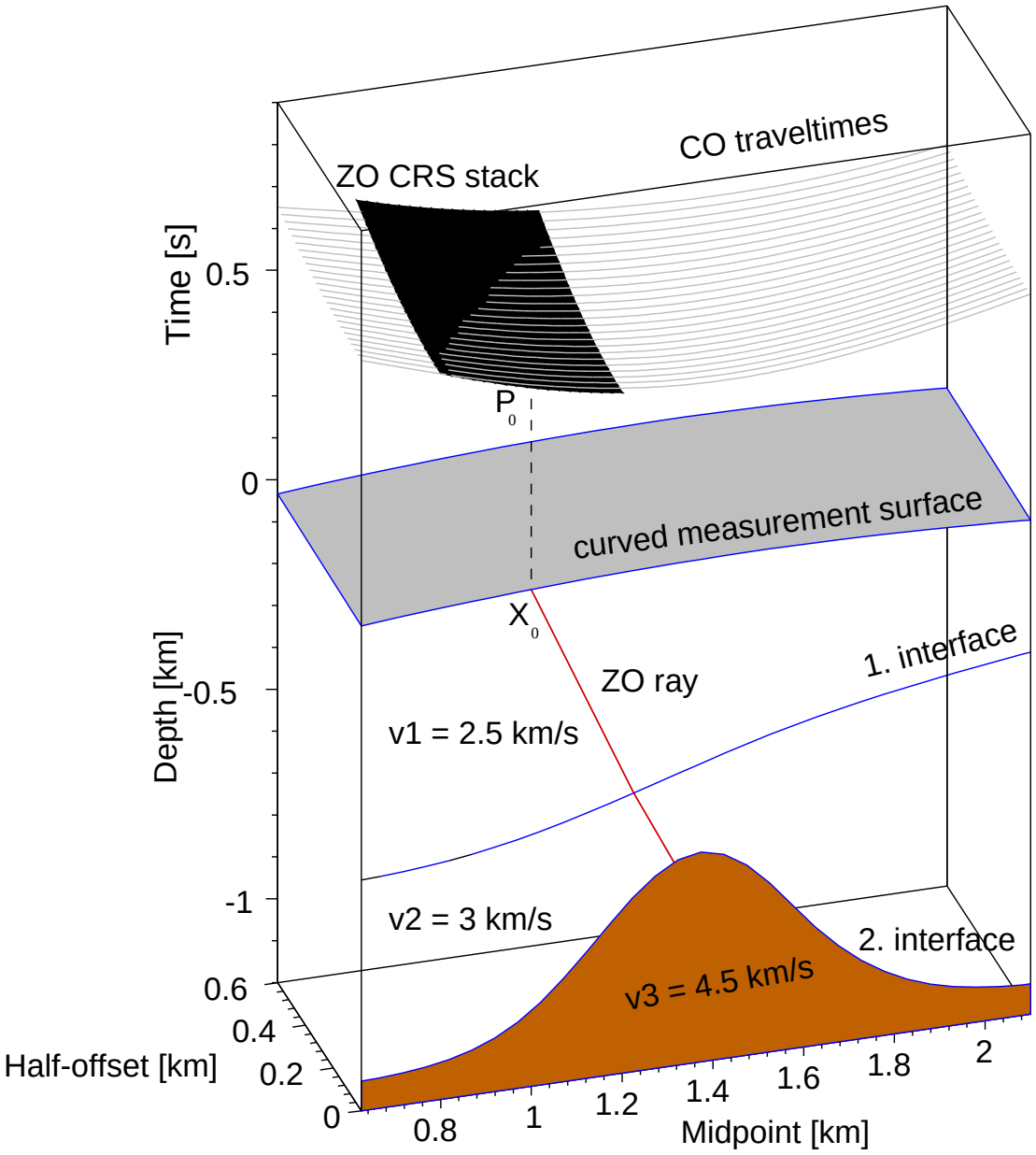

Figure 3: Lower half (front): a 2D medium with three constant-velocity layers. Upper half: Common-Offset (CO) traveltime curves of the prestack data. The black surface corresponds to the zero-offset CRS stack operator for a curved measurement surface.

The subscripts T and H denote the tangent dipping and horizontal measurement surface respectively. The latter transformation results from using $\beta_S = \beta_S^* - \alpha_S^*$.

SYNTHETIC DATA EXAMPLE

Let us consider the depth model of Figure 4 with four horizontal reflectors and a free measurement surface given by a circular arc with radius $r_S = 1/K_S = 10$ km and the apex at $x = 3.5$ km. The propagation velocities are for (P) compressional waves in every layer. At various points SG on the curved measurement surface with an interval $\Delta x = 0.05$ km, we calculated by ray tracing t_0, β_S^* and K_{NIP}. They determined the hyperbolic moveout (eq. 5) for each primary reflection, which provided the v_{NMO} values given by formula (7). The NMO velocity v_{NMO} (eq. 7) for each reflector as a function of the horizontal coordinate x is shown as the dotted line in Figure 5.

The transformed velocities $v_{NMO,T}$ (eq. 10) and $v_{NMO,H}$ (eq. 11) for each reflector also are shown in Figure 5. As they relate to planar measurement surfaces we can call upon existing algorithms (Dürbaum, 1954; Dix, 1955; Shah, 1973; Hubral and Krey, 1980) to recover arbitrarily layered constant-velocity 2D subsurface models provided the pair $(v_{NMO,H}, t_0)$ is given along the curved measurement surface with respect to each primary reflection.

In the following we have confined ourselves only to the indicated model of Figure 4 with horizontal reflectors. In this case the inversion strategy for the curved measurement surface reduces to the familiar standard Dix inversion. This results from transforming v_{NMO} at SG on the curved surface to $v_{NMO,H}$ as indicated above. It is obvious that for the i-th primary reflection we have for $v_{NMO,H}^2$ the familiar expression (Dix, 1955)

$$v_{rms,i}^2 = \frac{v_1^2\ \Delta t_1 + v_2^2\ \Delta t_2 + ... + v_i^2\ \Delta t_i}{t_{0,i}}\ , \quad i = 1, ..., N\ , \tag{12}$$

v_i is the velocity in layer i, $t_{0,i}$ is the two-way traveltime to interface below layer i and $\Delta t_i = t_{0,i} - t_{0,i-1}$, is the two-way traveltime in layer i.

We can therefore compute the interval velocity of layer i from the well known formula

$$v_i = \left[\frac{v_{rms,i}^2\ t_{0,i} - v_{rms,i-1}^2\ t_{0,i-1}}{t_{0,i} - t_{0,i-1}}\right]^{1/2}\ , \tag{13}$$

and the thickness of layer i from

$$\Delta z_i = v_i\ \frac{\Delta t_i}{2}\ . \tag{14}$$

In this way we can recover the exact or true interval velocities shown in Figure 6 and the exact depth model shown in Figure 4 and Figure 7 as denoted by the continuous lines. To be more realistic, we computed however by ray tracing the stacking velocities from simulated CMP gathers for primary reflections recorded on the curved measurement surface with the half-offset $h_{MAX} = 1$ km. This we did by fitting a straight line to the $t^2(h^2)$ trajectory of the CMP gather. We then assumed in the above Dix-type inversion the computed stacking velocities on the curved measurement surface to be expressible by the analytic NMO-velocity (eq. 7). In this way we recovered the model indicated by the dotted lines (Figure 7).

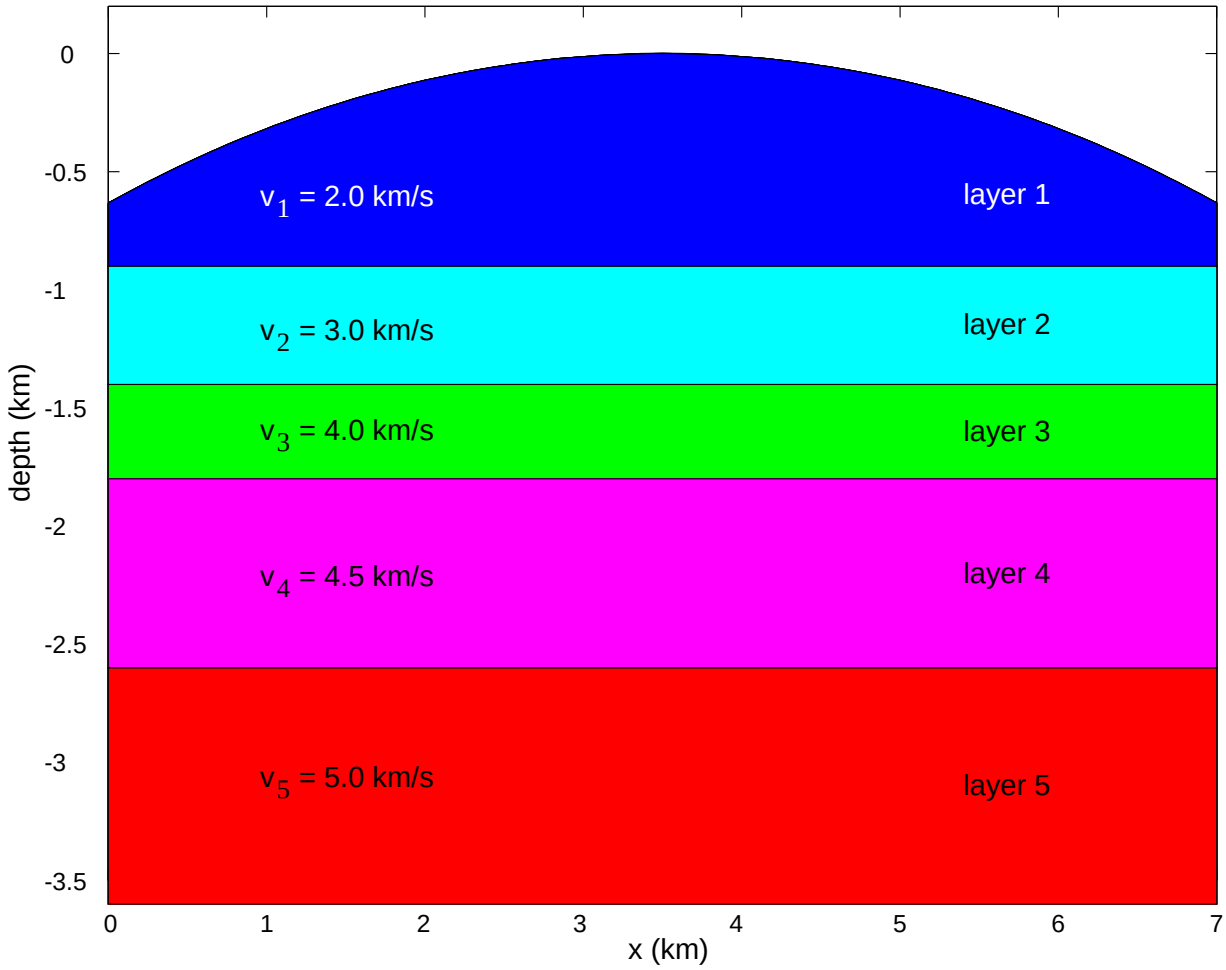

Figure 4: 2D model constituted of five plane parallel horizontal isovelocity layers.

Would we have performed the inversion with the above standard Dix algorithm, however assuming that the stacking velocities along the curved surface are equal to v_{rms} then we would have recovered the interval velocities and the depth model indicated by the crosses. Would we have assumed that the stacking velocities can be analytically expressed by $v_{NMO,T}$ then we would have recovered the model indicated by the circles. We can observe that there are significant errors that result from neglecting the curvature and dip of the measurement surface.

CONCLUSIONS

In this paper we have formulated a new analytic moveout formula (4) for a 2D curved measurement surface. It may find application, as indicated, in a number of modeling, inversion and stacking problems. The formula was derived for a 2D laterally inhomogeneous velocity model. It is in fact also valid for a 3D earth model with a curved measurement surface, provided all parameters in the 2D formula represent those in the plane defined by the tangent to the seismic line and the emerging normal ray at SG. We also demonstrated that the new normal moveout velocity

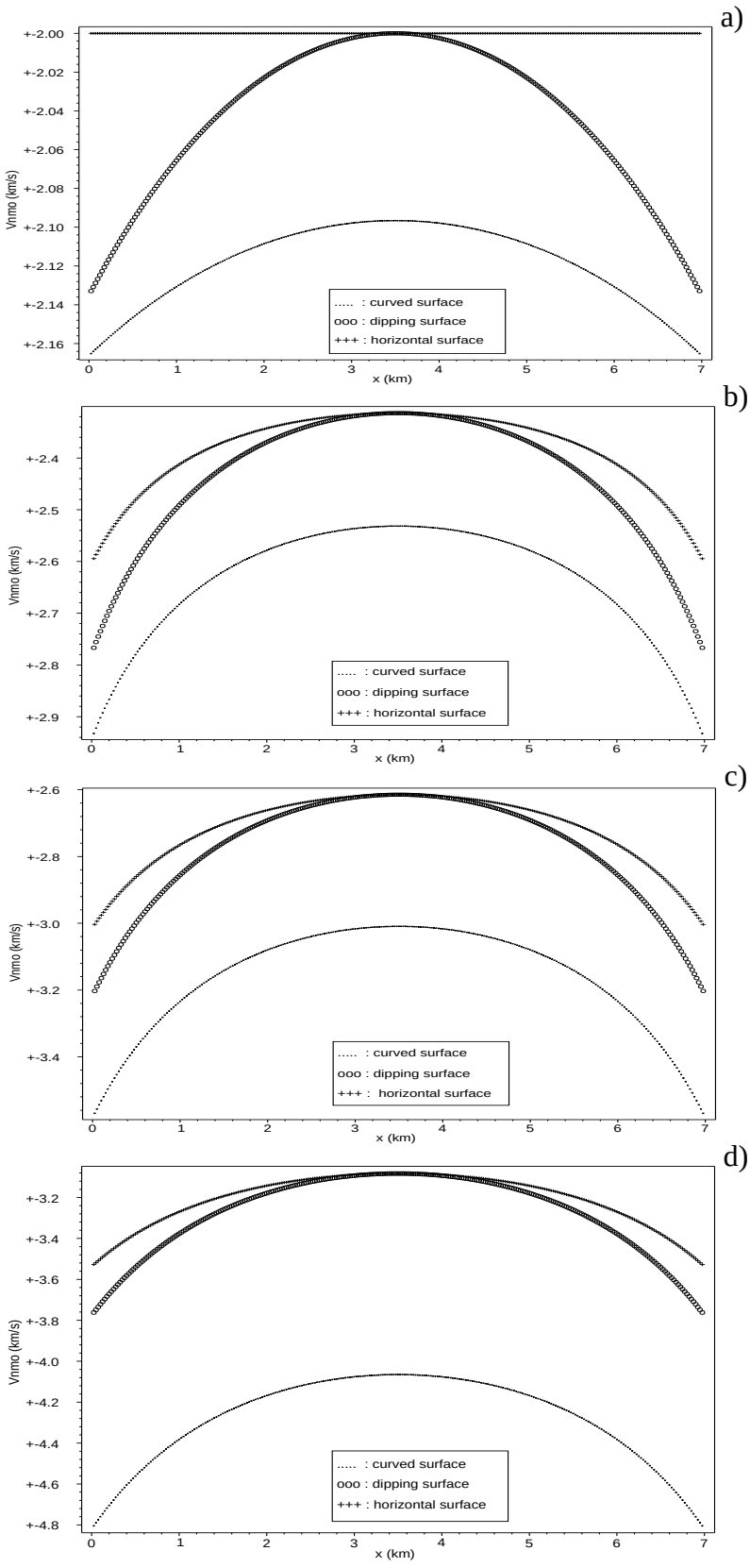

Figure 5: Three different NMO velocities for a)first reflector, b)second reflector, c)third reflector and d)fourth reflector.

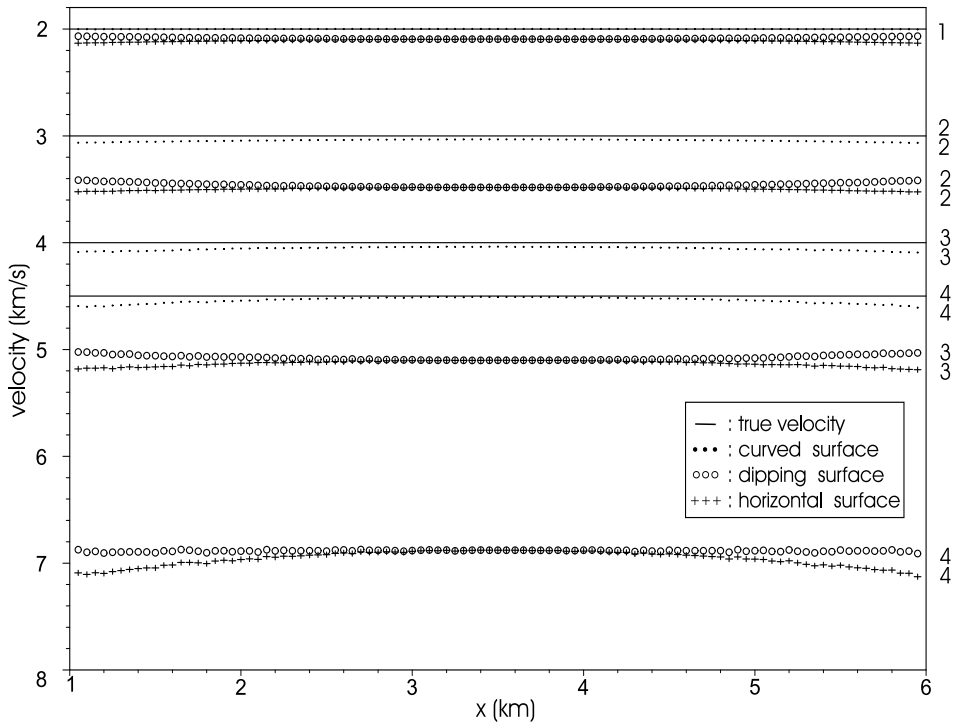

Figure 6: Four recovered interval velocities for the model of Figure 4.

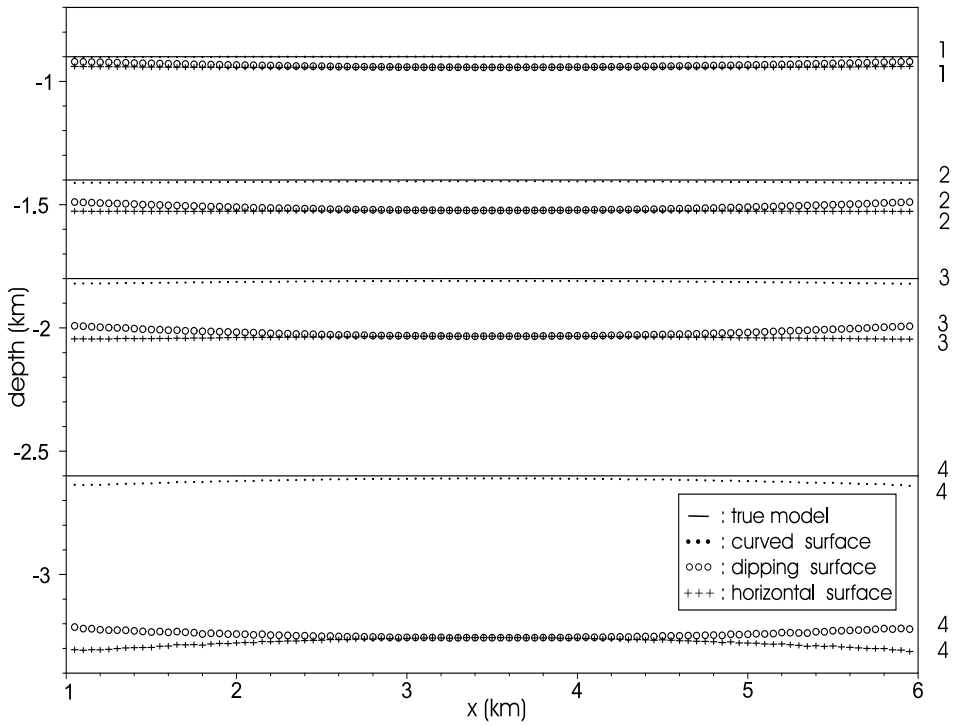

Figure 7: Recovered model obtained from stacking velocities and two-way times.

(eq. 7), which considers the surface topography, is much more exact than the NMO velocities for planar measurement surfaces if it comes to recover the interval velocities and the depths of the reflectors with a Dix-type inversion.

ACKNOWLEDGMENTS

The authors like to thank Alex Müller for his collaboration.

REFERENCES

Bortfeld, R. (1989). Geometrical ray theory: rays and traveltimes in seismic system (second order approximation of the traveltimes). *Geophysics*, 54:342–349.

Červený, V. (2001). Seismic ray theory. *Cambridge University Press.*

Chira, P. and Hubral, P. (2001). Moveout formulas for a curved 2D measurement surface and near-zero-offset primary reflections. *Submeted to Geophysics.*

de Bazelaire, E. (1988). Normal moveout revisited-inhomogeneous media and curved interfaces. *Geophysics*, 53:143–157.

de Bazelaire, E. and Viallix, R. J. (1994). Normal moveout in focus. *Geophys. Prosp.*, 42:477–499.

Dix, H. C. (1955). Seismic velocities from surface measurements. *Geophysics*, 20:68–86.

Dürbaum, H. (1954). Zur Bestimmung von Wellengeschwindigkeiten aus Reflexionsseismischen Messungen. *Geophys. Prosp.*, 2:151–167.

Fomel, S. and Grechka, V. (1998). On non-hyperbolic reflection moveout in anisotropic media. *Stanford Exploration Project, Technical Report 92*.

Gelchinsky, B., Berkovitch, A., and Keydar, S. (1999a). Multifocusing homeomorphic imaging. Part 1. Basic concepts and formulas. Special Issue: Macro-Model Independent Seismic Reflection Imaging. *J. Appl. Geophys.*, 42:229–242.

Gelchinsky, B., Berkovitch, A., and Keydar, S. (1999b). Multifocusing homeomorphic imaging. Part 2. Multifold data set and multifocusing. Special Issue: Macro-Model Independent Seismic Reflection Imaging. *J. Appl. Geophys.*, 42:243–260.

Hubral, P. (1983). Computing true amplitude reflections in a laterally inhomogeneous earth. *Geophysics*, 48:1051–1062.

Hubral, P. (1999). Special issue: Macro-model independent seismic reflection imaging. *Journal of Applied Geophysics*, 42:Nos. 3,4.

Hubral, P. and Krey, T. (1980). Interval velocities from seismic reflection time measurements: Monograph. *Soc. Expl. Geophys.*

Jäger, R., Mann, J., Höcht, G., and Hubral, P. (2001). Common reflection surface stack: Image and attributes. *Geophysics*, 66:97–109.

Müller, T., Jäger, R., and Höcht, G. (1998). Common reflection surface stacking method - imaging with an unknown velocity model. In *Expanded Abstracts*, pages 1764–1767. Soc. Expl. Geophys.

Schleicher, J., Tygel, M., and Hubral, P. (1993). Parabolic and hyperbolic paraxial two-point traveltimes in 3d media. *Geophys. Prosp.*, 41:495–513.

Shah, P. (1973). Use of wavefront curvature to relate seismic data with subsurface parameters. *Geophysics*, 38:812–825.